

UCLA

UCLA Electronic Theses and Dissertations

Title

Aryl Hydrocarbon Receptor-Mediated Induction of CYP1A1 and CYP1B1 Enzymes in Brain: A Preliminary Exploration of the Role of Oxylipins in Lung Cancer Metastasis to Brain

Permalink

<https://escholarship.org/uc/item/93d87590>

Author

tong, zhen

Publication Date

2020

Peer reviewed|Thesis/dissertation

UNIVERSITY OF CALIFORNIA

Los Angeles

Aryl Hydrocarbon Receptor-Mediated Induction of CYP1A1 and CYP1B1 Enzymes in
Brain: A Preliminary Exploration of the Role of Oxylipins in Lung Cancer Metastasis to
Brain

A thesis submitted in partial satisfaction
Of the requirements for the degree of Master of Science
In Environmental Health Sciences

by

Zhen Tong

2020

© Copyright by

Zhen Tong

2020

ABSTRACT OF THE THESIS

Aryl Hydrocarbon Receptor-Mediated Induction of CYP1A1 and CYP1B1 Enzymes in Brain: A Preliminary Exploration of the Role of Oxylipins in Lung Cancer Metastasis to Brain

by

Zhen Tong

Master of Science in Environmental Health Sciences

University of California, Los Angeles, 2020

Professor Oliver Hankinson, Chair

Lung cancer is one of the most frequent diagnosis cancers in the U.S. Importantly, primary lung cancer frequently metastasizes to the brain, but the survival and treatment of lung cancer brain metastasis are both poor. Aryl Hydrocarbon Receptor (AHR) mediated induction of Cytochrome P450 enzymes has been linked to cancer progression via binding to AHR agonists like 2, 3, 7, 8-tetrachlorodibenzo-p-dioxin

(TCDD). The exposure of TCDD significantly increases CYP 1A1 and CYP 1B1 in the lung and liver.

The western diet typically contains a high ratio of omega-6 (ω -6) to omega-3 (ω -3) polyunsaturated fatty acids (PUFA). Recently, our group has demonstrated that the action of ω -6 and ω -3 PUFA metabolism on tumor progression is an AHR dependent process. TCDD promotes tumor growth and metastasis under ω -6 enriched diets but inhibits tumor growth and metastasis under ω -3 enriched diets. This finding indicates that TCDD impact on lung cancer progression can be modified by dietary PUFA. Based on this new research ground, it is also interesting to evaluate TCDD's action on primary lung cancer metastasis to brain depending on different ratio of ω -6 to ω -3 PUFA in diet. We hypothesized that the lung tumor increases the metastasis to brain through an AHR agonist like TCDD, which induce the expression of some cytochrome P450 in the brain of the mice that were fed with rich- ω 6 diet.

To evaluate our hypothesis, we performed immunohistochemistry, digital pathology, RT-PCR, and liquid chromatography with tandem mass spectrometry. Our data demonstrated that the brain metastasis was found in mice fed with rich- ω -6 diet in mice treated with TCDD as compared with untreated mice. Further, TCDD significantly induced CYP 1A1 and CYP 1B1 in mice brain tissue under ω -6 enriched diet. In addition, the levels of oxylipins in plasma demonstrated that epoxides 5,6 EET are increases after TCCD treatment, as well as various diols like 5,6-DiHETrE, 11,12-DiHETrE, and 14,15-DiHETrE.

These results provide us a future research direction on combining effects of diets and environment carcinogens to analyze the mechanism to be involved in the metastasis to brain from the lung tumor cells.

The thesis of Zhen Tong is approved by

Michael Collins

Jesus A. Araujo

Oliver Hankinson, Committee Chair

University of California, Los Angeles

2020

Acknowledgment

At first, I would appreciate the mentoring from Dr. Oliver Hankinson, Dr. Sara Huerta-Yepez, and Dr. Michael Collins throughout my master's program at UCLA. I also appreciate Dr. Huerta-Yepez's help on my thesis revision. I learn many skills in research from them. I also want to say thank you to Dr. Jesus Araujo to be my thesis committee member.

RT-PCR and immunohistochemistry were done in Dr. Huerta-Yepez lab in Mexico. I appreciate the help from Dr. Huerta-Yepez, Dr. Ana Tirado-Rodriguez, Mayra Montecillo and Mario Morales.

The oxylipin analysis part was done by Dr. Hammack lab at UC Davis. I would thank them for the tissue and plasma oxylipin data generation.

Table of Contents

1. Introduction	1
1.1 Hypothesis	1
1.2 Background	1
1.2.1 Lung cancer statistics.....	1
1.2.2 Aryl Hydrocarbon Receptor (AHR) mediated induction of Cytochrome P450 in cancer.....	1
1.2.3 Omega 3/omega-6 PUFAs on cancer.....	3
1.2.4 Combined dietary and environmental effect on cancer progression.....	5
1.2.5 AHR agonists may reduce or enhance cancer progression based on dietary context.....	6
2. Materials and method.....	7
2.1 Chemicals	7
2.2 Cell lines and cell culture assays.....	7
2.3 Mouse husbandry and feeding	7
2.4 Mouse tumor models.....	8
2.5 Real Time Reverse transcription PCR.....	10
2.6 Hematoxylin and eosin stain	10
2.7 Immunohistochemical (IHC) Analysis.....	11
2.8 Tissue and LC/MS/MS analysis.....	11
2.9 Statistical analysis.....	12
3. Results.....	12
3.1 TCDD induced tumor brain metastasis from lung	12
3.2 TCDD induced CYP 1A1 and CYP 1B1 in brain	16
3.3 TCDD and EPHX2 in brain.....	17
.....	18
3.4 Oxylipins level change in mice plasma	18
4. Discussions.....	20
4.1 Key findings	20
4.2 Limitations and future work	22
5. Conclusions and implications	23
6. References	25

Table of Figures

Figure 1. TCDD chemical structure	2
Figure 2. TCDD and AHR binding	3
Figure 3. PUFAs metabolic pathways.	5
Figure 4. Overall research justification.	6
Figure 5. Experimental model.	14
Figure 6. Mice fed with rich- ω 6 diet and treated with TCDD shown metastasis to brain.....	15
Figure 7. TCDD induction of CYP 1A1 in mice fed with rich- ω 6 diet.	16
Figure 8. TCDD induction of CYP 1B1 in mice fed with rich- ω 6 diet.	17
Figure 9. Expression of EPHX2 in mice treated with TCDD and fed with rich- ω 6 diet.....	18
Figure 10. EPHX2 expression in male and female mice brain..	18

List of tables

Table 1. Levels of oxylipin change in plasma.	19
--	----

1. Introduction

1.1 Hypothesis

The hypothesis is that the lung tumor increases the metastasis to brain through, an AHR agonist like TCDD, which induce the expression of some cytochrome P450 in the brain of the mice that were fed with rich- ω 6 diet.

1.2 Background

1.2.1 Lung cancer statistics

Lung carcinoma is one of the most common diagnosis cancers in the U.S¹. Despite the overall trending of declining due to the advancement of modern medicine, lung cancer remains one of the lowest survival rates alone with liver cancer and pancreatic cancer¹. In addition, It has been found that lung cancer in human patients frequently metastasizes to the brain². The prognosis and the median survival of patients with lung cancer metastasis to the brain are both poor due to the rapid disease progression and limited treatment.

1.2.2 Aryl Hydrocarbon Receptor (AHR) mediated induction of Cytochrome P450 in cancer

Aryl Hydrocarbon Receptor (AHR) is a nuclear receptor and numerous literature demonstrated that AHR is expressed in a broad pattern in different tissues of vertebrates, including different compartments of the brain^{3,4}.

2, 3, 7, 8-tetrachlorodibenzo-p-dioxin (TCDD) is a common AHR ligand as well as an environmental pollutant (**Figure 1**).

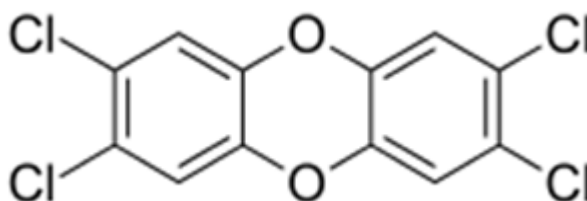


Figure 1. TCDD chemical structure⁵

Although the exact mechanism of action of TCDD to cause cancer is still unclear, the Aryl Hydrocarbon Receptor (AHR) has been proved to be the receptor of TCDD⁶. After binding to TCDD, the AHR translocated into the nucleus to bind to a specific DNA sequence as a transcription factor, activating transcription for some essential genes, including CYP1A1 and CYP1B1 in many tissues in all mammals (**Figure 2**)⁷⁻¹⁰. Because research has proved that TCDD can distribute in many different organs like lung, liver, and brain, the AHR in brain could potentially be activated^{8,11,12}. The induction of CYP 1A1 and CYP 1B1 enzymes in lung and liver has been linked to tumor growth, angiogenesis, and metastasis^{8,13}.

In addition, previous research has shown that TCDD and some other AHR agonists like indole and polychlorinated biphenyls (PCBs) can both increase or inhibit tumor growth in mice models^{14,15}.

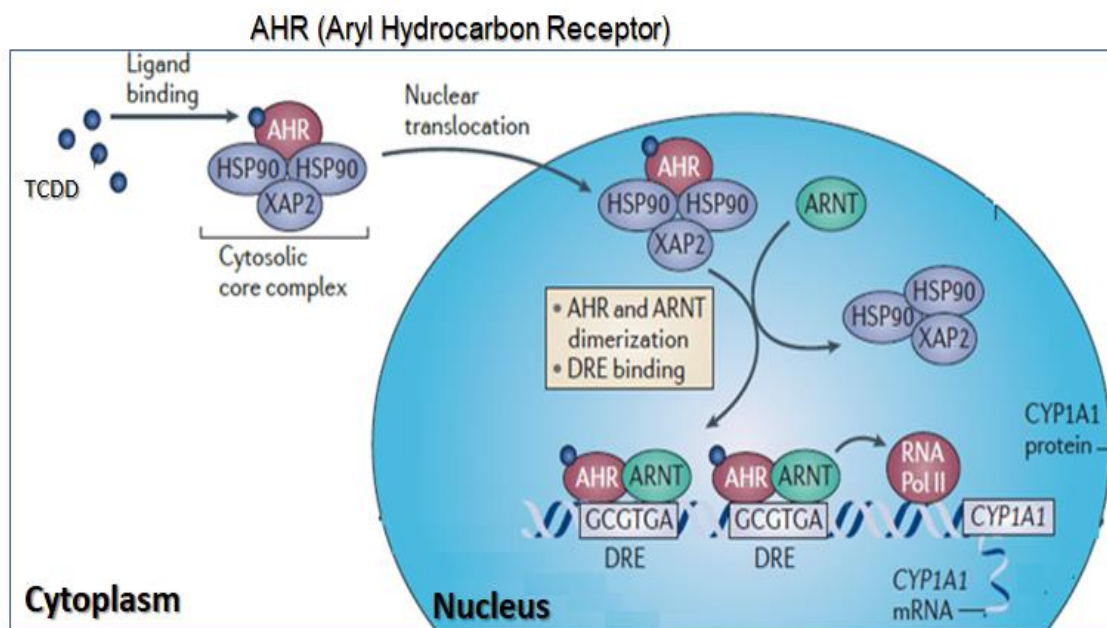


Figure 2. TCDD and AHR binding⁹

1.2.3 Omega 3/omega-6 PUFAs on cancer

Dietary effects on health have been heavily studied. Among past studies, typical western diet compositions, which is described as high intake of omega-6 (ω -6) polyunsaturated fatty acids (PUFA) with the ω -6/ ω -3 ratio of 20:1 like arachidonic Acid (ARA, C20:4, ω 6) and linoleic (L.A., C18:2, ω 6) acid, have drawn the linkage to adverse health effects like cancers¹⁶. In contrast with ω -6 PUFAs, omega-3 (ω -3) PUFAs, like eicosapentaenoic Acid (EPA, C20:5, ω 3), and docosahexaenoic acid (DHA, C22:6, ω -3), have been associated with beneficial health effects¹⁷. The metabolism of PUFA can be classified into three major pathways: the cyclooxygenase pathway, cytochrome P450 pathway, and lipoxygenase pathway (**Figure 3**)¹⁸. Within the cytochrome P450 pathway, CYP 1A1 and CYP1B1 are essential enzymes that metabolize PUFA into epoxides, which are further metabolized into diols via epoxide hydrolase enzyme (EPHX2)¹⁹. It

has been demonstrated that EPHX2 expression varies between males and females due to the estrogen-dependent epigenetic regulation²⁰. This difference of EPHX2 expression would potentially lead to different health outcomes between sex when feeding with the same dietary PUFA¹³. Experiments have shown that increasing the level of ω -6 PUFAs epoxides promotes cancer progression. On the other hand, the high level of ω -3 PUFAs epoxides presented an inhibitory effect on cancer progression¹⁷. The use of the epoxide hydrolase inhibitor will be important in our experiment because the conversion of epoxide to diols via EPHX2 is a rapid process²¹. Reducing the activity of EPHX2 would be necessary to investigate PUFA epoxides. Different oxygenated metabolites of PUFAs, known as oxylipins, play essential roles in our bodies. However, some of the oxylipins are positively related to the progression of cancer and metastasis²²⁻²⁷. A bulk of published literature focuses on how oxylipins (prostaglandins and lipoxins) affect primary brain cancer like glioblastoma as well as metastatic melanoma; however, the pathways that are involved are primarily Cyclooxygenase and Lipoxygenase pathways^{24,25,28-31}. The cytochrome P450 pathway is not extensively studied in primary brain cancers, but some literature has found that under the cytochrome P450 pathway, one of the Arachidonic Acid (ARA) metabolites, called 20-HETE (20-Hydroxyeicosatetraenoic Acid), participate in breast cancer metastasis²³. Epoxyeicosatrienoic acids (EETs), which are ARA metabolites from CYP pathway, have been discovered to be mitogenic and angiogenic in the brain³². Previous studies have shown that TCDD-treated mice were experiencing changes of oxylipins in both lung and liver⁸. More specifically, elevated levels of certain EETs in xenograft cancer cells promote tumor growth and metastasis^{33,34}. Thus, in order to investigate the influence of

TCDD-induced oxylipins in metastatic cancer to brain, either brain tissue oxylipins or plasma oxylipins quantification is needed. However, the research about how EETs involved in lung cancer metastasis to brain is still limited.

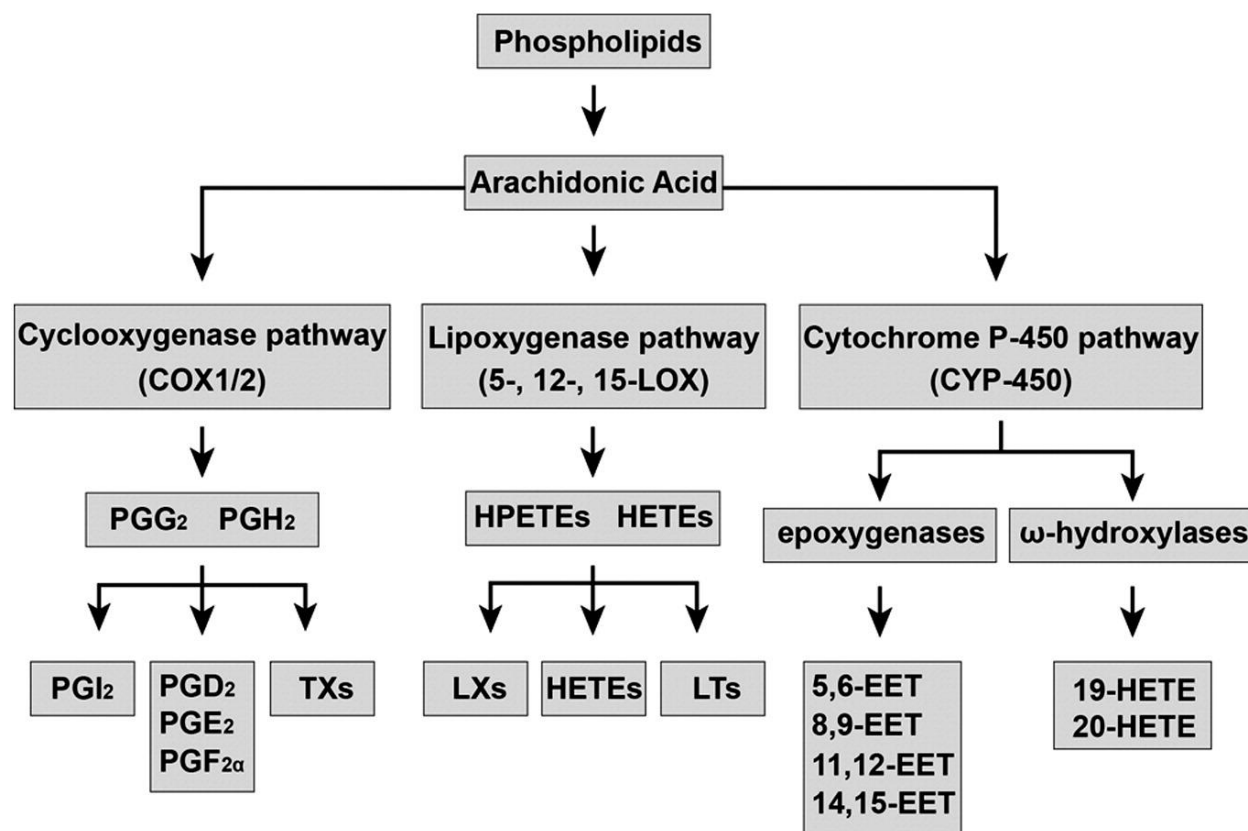


Figure 3. PUFAs metabolic pathways¹⁸. Three enzymatic pathways metabolize arachidonic Acid into different metabolites including P.G.s (Prostaglandins) by COX, HETEs (Hydroxyeicosatetraenoic acids) by LOX and epoxides by CYP-450.

1.2.4 Combined dietary and environmental effect on cancer progression

We are exposing to different types of environmental carcinogens daily, so it is crucial to consider the combined effects of diets and environmental factors on cancer progression (**Figure 4**). As previously mentioned, TCDD as a common environmental pollutant, and

AHR ligand can activate AHR constantly, which in turn activates the PUFA metabolism pathway of CYP450. This research justification would be valuable to have a deeper understanding of PUFA dietary effects on cancer and even dietary treatment of cancer.

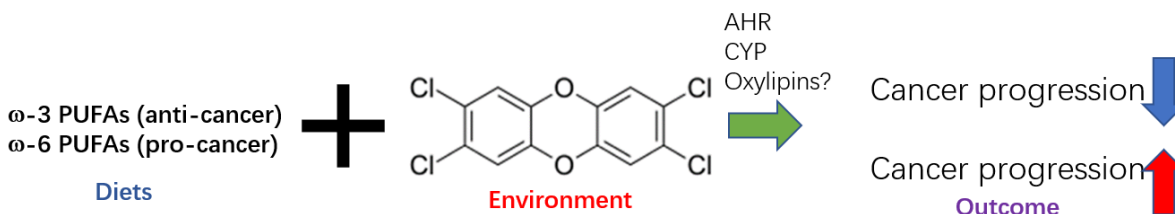


Figure 4. Overall research justification. Diets components and environmental components are combining to influence cancer progression. This paper focuses on PUFAs and TCDD in brain metastasis from lung cancer cells.

1.2.5 AHR agonists may reduce or enhance cancer progression based on dietary context

In the most recent published paper, our group has demonstrated that environmental AHR agonists, such as TCDD, may decrease or promote lung cancer progression depending on the different composition of PUFA intake¹³. Specifically, TCDD declined the tumor growth and metastasis to lung and liver in ω -3 fed mice, whereas the opposite results can be observed in ω -6 fed mice¹³. Based on this finding, it is also interesting to see if the same effects of TCDD on lung cancer metastasis to brain can also be repeated depending on the different ratios of ω -6 to ω -3 PUFA intake.

2. Materials and method

2.1 Chemicals

TCDD (>99.99% purity) was purchased from Dow Chemical's Co. (Midland, MI, USA), and dissolved in 1,4-Dioxane (New Haven, Connecticut), and stored in the dark at -20°C . 1-Trifluoromethoxyphenyl-3-(1-propionylpiperidin-4-yl) urea (TPPU) was made based on the previously published work³⁵.

2.2 Cell lines and cell culture assays

Lewis lung carcinoma cell line (LLC) (ATCC #CRL-1642™) was purchased from American Type Culture Collection (Manassas, VA). Cells were cultured in alpha Minimal Essential Medium (α -MEM) (Gibco, Carlsbad, CA). LLC cell lines were given 10% fetal bovine serum (FBS, Omega Scientific, Tarzana, CA) and penicillin-streptomycin (P/S, Gibco) plus Fungizone. *In vivo* injection step, LLC cells were harvested from sub-confluent cultures by using 0.05% trypsin-EDTA and then neutralized with cell culture medium at 4°C . Prior to re-suspension in serum-free alpha medium, the cells were washed three times in serum-free medium.

2.3 Mouse husbandry and feeding

C57BL/6 male mice at 5-weeks-old of age were purchased from the Jackson Laboratory (Bar Harbor, Maine). The mice were set up five per cage under the maintenance of UCLA DLAM of 3v vivarium, according to the ethical guidelines for animal handling

required by the UCLA Institutional Animal Care and Use Committee (IACUC). Each cage is ventilated with constant room temperature between 20°C-22°C. The mice room was provided with a 12-hour light and 12 hours dark cycle. The mice were fed with NIH-31 open Formula Mouse/Rat diet 7013 from Envigo, Madison, Wisconsin (referred to as normal chow in this paper). After 72 hours of mice arrival, they were fed with either ω -3 enriched diets (referred to as diet 29) or ω -6 enriched diets (indicated as diets 21). The ω -3 rich diet (diet 29) had a ω -6/ ω -3 ratio of 1.1:1 (theoretical) and 1.5:1 (experimental) with 1% of PUFA content. The ω -6 enriched diet (diet 21) had the ω -6/ ω -3 ratio of 20:1, which is highly similar to the real-life western diet ratio of ω -6/ ω -3. Mice consumed equal amounts of calories per day on each diet, and the food was changed twice per week. These special diets were modifications of the AIN-93G mouse diet. Special diets were formulated to contain 3.8 Kcal/g with 19% of calories from protein (casein), 64% from carbohydrates, and 17% from fat (Envigo Teklad, Madison WI). Since polyunsaturated fatty acids are easily oxidized if exposed to air, the diets were stored in vacuum-sealed pouches at -80°C unless used. Water was provided ad libitum.

2.4 Mouse tumor models

The mice were randomly separated into two groups. They were fed with experimental diets and ad libitum for three weeks before the injection of cells. TPPU was added to the water and changed twice a week. TCDD was injected intraperitoneally with a concentration of 40 μ g/kg for the initial injection and 10 μ g/kg for the sequential

injections once a week. 1,4-Dioxane was selected as a solvent of TCDD instead of corn oil because corn oil content may affect the results of this diet study. The LLC cells were injected into the mice subcutaneously with 2×10^5 cell count. Two weeks after the injection of LLC cells, tumor growth was measured by an electronic Vernier caliper every other day until the termination of the experiment or until resection of the tumor. The dead mice were excluded from the data collection (4 out of 48 total). Tumor volumes were calculated from the formula: $\text{volume} = (\text{the shortest diameter})^2 \times (\text{the largest diameter}) / 2 \times (4.19)^{36}$. After the tumor reached a certain size calculated by the formula above, resection surgery was performed, and the wounds were closed by surgical stamps. Half of the tumors were stored in liquid nitrogen, and another half were put in formalin for histology use. Tumors were weighed right after resection. For the post-op care, Gabapentin (100 mg/kg orally) plus carprofen (5 mg/kg subcutaneously) was used as analgesics immediately after surgery, daily thereafter for three days, and then as needed. Three to five weeks after the surgery, mice were sacrificed based on their health status. The plasma was first collected and put in tubes with anticoagulants. The lung and brain were extracted from the mice. The model is shown in **Figure 5**. For lungs, half was frozen in liquid nitrogen and stored at -80°C , and the other half was fixed in formalin saline for immunohistochemistry. The intact brain was cut by a sagittal plane. Half of the brain was frozen in liquid nitrogen and stored at -80°C . Another half was fixed in formalin saline (Fisherbrand, Pittsburg, PA), Torrance, CA). The experiments were approved by the UCLA Institutional Animal Care, and Use Committee (IACUC), and the daily care and maintenance were followed based on guidelines.

2.5 Real-Time Reverse transcription PCR

From each frozen tissue, the RNA was extracted by using the Trizol and chloroform. Then 1 µg of RNA was used for cDNA synthesis in a volume of 20 µL. The presence of messenger RNA (mRNA) of CYP 1A1, CYP1B1, and EPHX2 was determined from total cDNA extracts obtained by miRneasy kit (QIAGEN). For RT-PCR, the Universal Taqman Master Mix II kit (Applied biosystems) was used. Taqman probes (CYP 1A1, CYP1B1, and Tubulin) and Taqman Universal Master Mix were used (Applied Biosystems). In addition, as control of expression, the Tubulin transcription was evaluated. The relative value of expression of the genes was calculated using the method $2^{-(\Delta\Delta Ct)}$ comparing the expression of mRNA of CYP 1A1, CYP1B1, and EPHX2 related to Tubulin as an endogenous control. The RT-PCR was run in an Applied Biosystems 7500 real-time PCR machine.

2.6 Hematoxylin and eosin stain

Tissues were used for Mayer's hematoxylin and eosin (H&E) for histopathological examination of metastasis. Briefly. Sections of 4 µm of tissue were dewaxed in xylol and rehydrated through a series of solvents (xylene, 100% ethanol, 90% ethanol, 70% ethanol, and distilled water). Subsequently, tissues were merged in hematoxylin for one minute, followed by three washes in ethanol-HCl, one wash in water, and one wash in 70% ethanol. After two minutes of treatment in eosin, the tissue was dehydrated under the following procedures: distilled water, 70% ethanol, 90% ethanol, 100% ethanol and xylene in baths with 5 minutes each. Lastly, the tissues were covered with resin and put

to dry at room temperature.

2.7 Immunohistochemical (IHC) Analysis

Slides from brain tumor tissue were used for Immunohistochemistry staining to detect CYP enzymes and EPHX2 protein.

For immunohistochemical analysis, paraffin-fixed tissues were cut into four μ m-thick sections blocks and stained by using the Vectastain Elite ABC HRP Kit (Vector; Burlingame, CA). Firstly, Sections were deparaffinized at 68 °C in xylene and dehydrated through three alcohol changes (100%, 90%, and 70% ethanol). Endogenous peroxidase blocking was in 3% hydrogen peroxide (hydrogen peroxide in methanol). Antigen retrieval was performed in 0.01M sodium citrate at 93 °C. Slides were incubated with primary antibodies overnight at room temperature against CYP1A1 (1:1000 dilution) and CYP 1B1 (1:1000 dilution) from Invitrogen (Carlsbad, CA), EPHX2 (1:1000 dilution) from Novus Biologicals (Littleton, CO).

Then, sections were incubated with the Vectastain Elite ABC HRP Kit Secondary Antibody and DAB detection system (Vector Laboratories, Burlingame, CA). The slides were counterstained with hematoxylin. Finally, the slides were dehydrated by increasing the concentration of ethanol and mounted with resin.

The pictures of stained slides were taken by using an Aperio ScanScope CS (Leica, Nussloch, Germany), which produces 40x digital images.

2.8 Tissue and LC/MS/MS analysis

Oxylipins extraction and the measurement via liquid chromatography with tandem mass

spectrometry were performed as described previously^{37,38}. Dr. Hammock group at UC Davis did the whole LC/MS/MS analysis. In short, plasma was put into liquid nitrogen. 10 μ L of antioxidant cocktail solution (0.2 mg/mL of butylated hydroxytoluene (BHT) and EDTA) and 10 μ L of 100 nM isotope internal standard solution (including d4 6-ketoPGF1 α , d4 PGE2, d4 TXB2, d4 LTB4, d11 14,15-DiHETrE, d4 9- HODE, d8 5HETE and d11 11(12) EpETrE) were added. The plasma was stored under -80°C overnight. The LC/MS/MS analyses were carried out on an Agilent 1200 SL UHPLC system (Santa Clara, CA) coupled with AB Sciex 4000 QTRAP system (Foster City, CA) under negative MRM mode.

2.9 Statistical analysis

The data was analyzed by a two-tailed student T-test to compare two independent groups through Excel 2016. The Graph Pad Prism Version 5.0 software (San Diego, CA) was used to construct the graphs. A Chi-square test was used via the Quantpsy website calculator. Levels of significance are indicated as follows: * $p < 0.05$, ** $p < 0.01$, *** $p < 0.001$.

3. Results

3.1 TCDD induced tumor brain metastasis from lung

Based on the LLC metastasis model, **Figure 5** presented H&E staining followed under different timeline. The mice were fed with a rich- $\omega 6$ diets and were exposed to TCDD

thought out the whole timeline. Roughly, about four weeks, we implanted the lung tumor and closely monitoring the size change. Primary tumor resection started when a certain size of the tumor is reached. The H&E staining analysis was presented at 20X magnification with darker red color in the TCDD group compared with the vehicle. Two weeks after the resection, we started to sacrifice the mice for the extraction of lung tissue. Metastasis in lung tissue was shown in 4X magnification. The larger area of dark red color in the TCDD treated group indicates more metastasis of LLC in lung tissue. At the same time of extracting the lung, we also collected the brain tissue. Black arrows on 20X magnification of brain H&E staining indicated more metastasis in brain tissue in the TCDD group in comparison with dioxane treated.

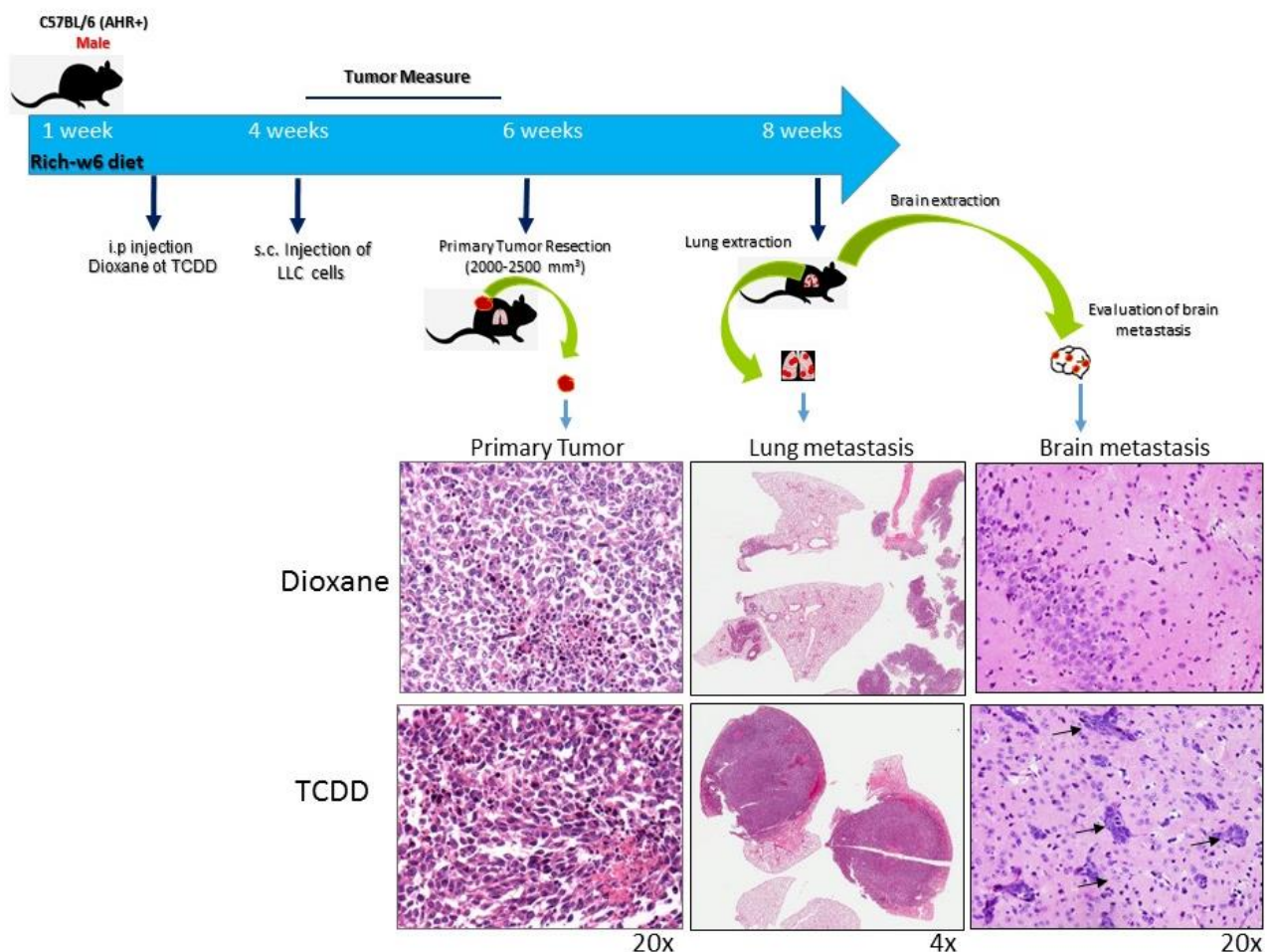


Figure 5. Experimental model. Based on the LLC metastasis model, this figure presented H&E staining followed under different timelines. The mice were fed with a rich- ω 6 diet and were exposed to TCDD throughout the whole timeline. Roughly about four weeks, we implanted the lung tumor and closely monitoring the size change. Primary tumor resection started when a certain size of the tumor is reached. The H&E staining analysis was presented at 20X magnification with darker red color in the TCDD group compared with the vehicle. Two weeks after the resection, we started to sacrifice the mice for the extraction of lung tissue. Metastasis in lung tissue was shown in 4X magnification. The larger area of dark red color in the TCDD treated group indicates more metastasis of LLC in the lung tissue of the TCDD group. At the same time of extracting the lung, we also collected the brain tissue. Black arrows on 20X magnification of brain H&E staining indicated more metastasis in brain tissue in the TCDD group in comparison with dioxane treated.

In **Figure 6**, we presented H&E staining for TCDD and dioxane treated groups. Black arrows indicated lung cancer cells metastasis to brain tissues. The 60X magnification on the right side of **Figure 6A** showed the histology of the lung cancer cells in brain tissue. The histology of the LLC metastasis in the brain was confirmed by an expert pathology from Mexican Children Hospital, Federico Gomez at Mexico City, Dr. Lourdes Cabrera. **Figure 6B and 6C** are the quantifications of the lung cells metastasis in brain. **Figure 6B** shows that among all the TCDD treated mice, 80% of them was found metastasis under H&E analysis. None of the dioxane treated mice has metastasis. In addition, **Figure 6C** is showing the details of how we calculate 80% in **Figure 6B**, as well as the Chi-square test result. $P = 0.018$.

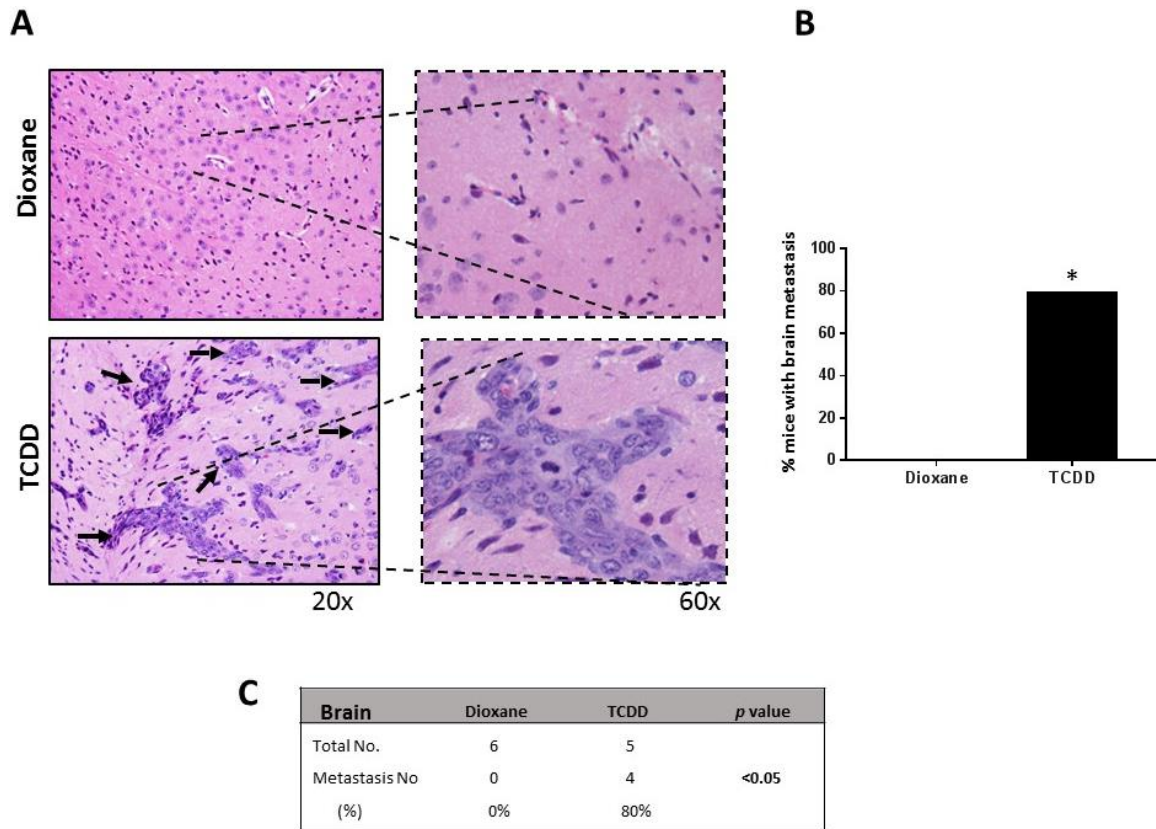


Figure 6. Mice fed with rich- ω 6 diet and treated with TCDD shown metastasis to brain. In the H&E staining for TCDD and dioxane treated groups fed with rich- ω 6 diet. The mice with brain metastasis were identified for an expert pathology. A. representative microphotographic 20 and 60x of brain tissue from mice treated or untreated with TCDD, and black arrows indicated lung cancer cells to metastases to brain tissues. B and C are the quantifications of the number of mice that presented lung cells metastasis in brain. B shows that among all the TCDD treated mice, 80% of them was found metastasis under H&E analysis. None of the dioxane treated mice has metastasis. C. Chi-square test result. * $p = 0.018$.

3.2 TCDD induced CYP 1A1 and CYP 1B1 in brain

CYP 1A1, CYP 1B1, and EPHX2 quantification in brain after TCDD treatment were done by both immunohistochemistry and RT-PCR. **Figure 7A** show representative microphotography of the immunohistochemistry of CYP 1A1 in brain tissue. The TCDD group presented more positive staining than the control group (dioxane). The IHC pictures were taken under 40x magnification. **Figure 7B** presents the RT-PCR of CYP 1A1 expression to Tubulin. TCDD treated brain tissue has a significant increase in the expression of CYP 1A1 in brain tissue compared with the dioxane group ($p<0.05$). **Figure 8A** representative microphotography of the immunohistochemistry of CYP 1B1 in brain tissue. The TCDD group presented more positive staining than the control group (dioxane), 40x magnification. **Figure 8B** presents the RT-PCR of CYP 1B1 expression. We used Tubulin as an endogen. TCDD treated brain tissue has a 15 times increase in the expression of CYP 1B1 in brain tissue compared with the dioxane group ($p<0.05$).

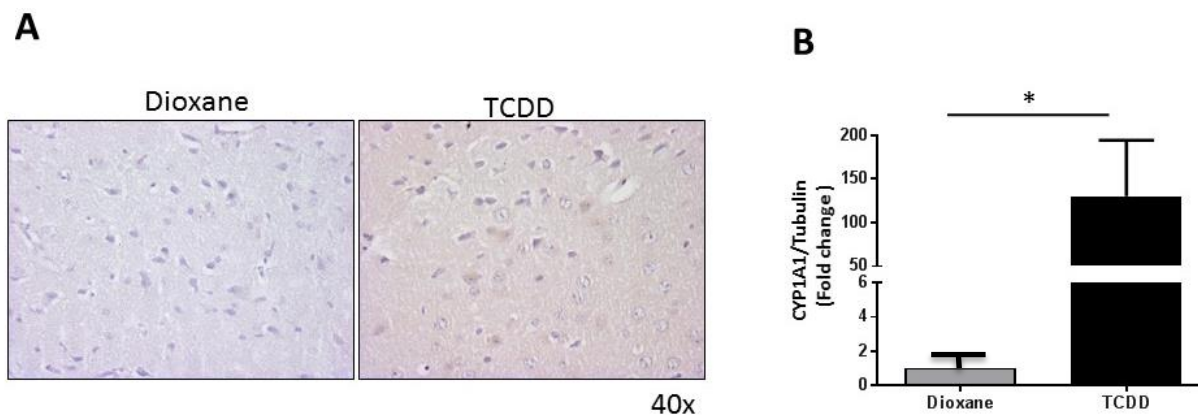


Figure 7. TCDD induction of CYP 1A1 in mice fed with rich- ω 6 diet. A. Immunohistochemistry staining between TCDD and dioxane (40x) (A). B. RT-PCR shows a significant increase in CYP1A1 expression to Tubulin in TCDD treated group, $*p<0.05$.

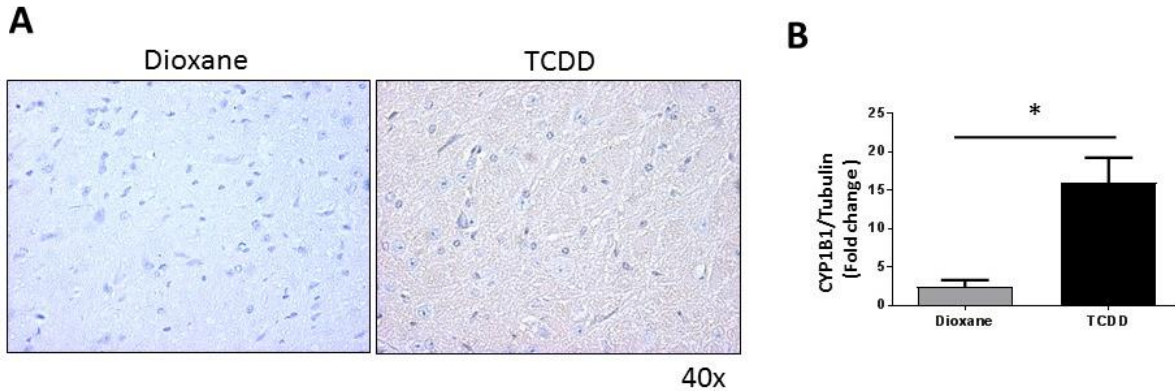


Figure 8. TCDD induction of CYP 1B1 in mice fed with rich- ω 6 diet. A. Immunohistochemistry staining between TCDD and dioxane (40x) (A). B. RT-PCR shows a significant increase in CYP1A1 expression to Tubulin in TCDD treated group, * $p < 0.05$.

3.3 TCDD and EPHX2 in brain

Both immunohistochemistry and RT-PCR results of EPHX2 expression in brain tissue after TCDD treatment are showing in Figures **9A** and **9B**. The immunostaining indicates some positive staining in TCDD treated mice, but the RT-PCR results did not show a significant difference of EPHX2 in mice brain tissue after TCDD treatment. ($p > 0.05$) Based on the previous finding that EPHX2 expression in the lung is different between male and female mice. We did the IHC to compare the expression in brain tissue between male and female mice under normal conditions (dioxane) (**Figure 10**). From the immunostaining, we found that in male brain tissue, there are more positive staining than in female brain tissue, which resembles the pattern of EPHX2 expression in lung tissue. However, RT-PCR analysis will be done later to confirm the finding from the immunohistochemistry assay.

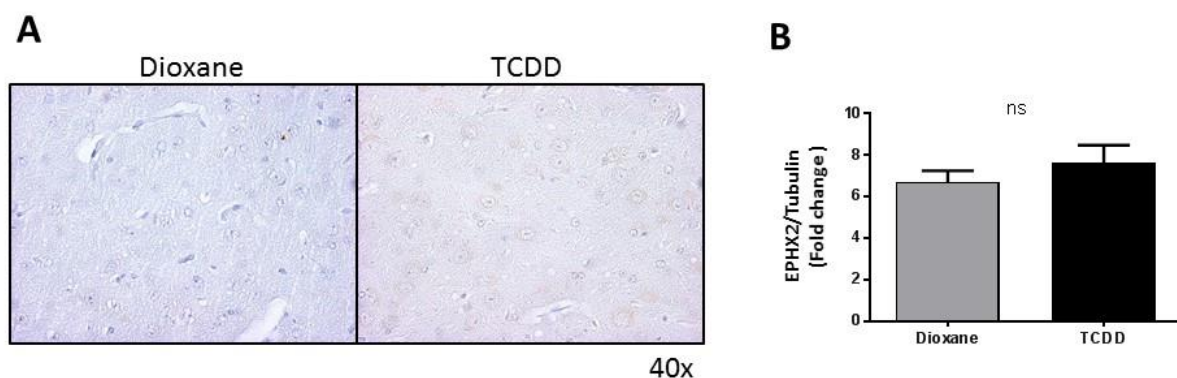


Figure 9. Expression of EPHX2 in mice treated with TCDD and fed with rich- ω 6 diet. A. Immunohistochemistry staining between TCDD and dioxane (40x) (A). B. RT-PCR shows not significantly different between TCDD treated and untreated mice. ns = not significant.

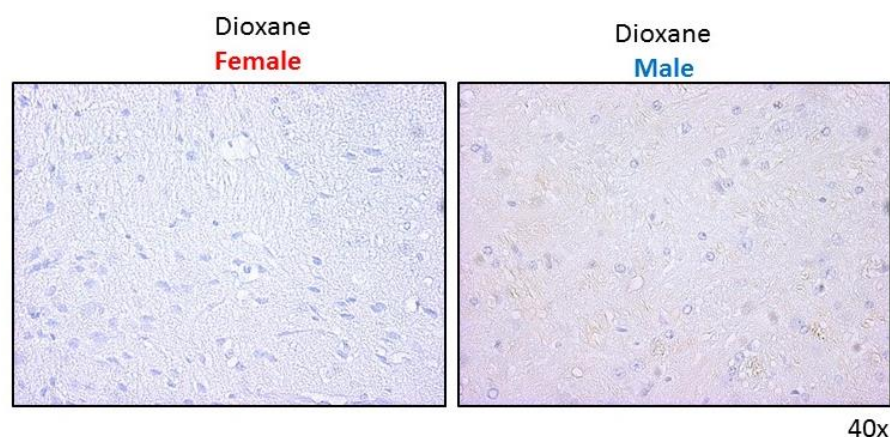


Figure 10. EPHX2 expression in male and female mice brain. The expression of EPHX2 was evaluated by immunohistochemistry in brain tissue from female and male mice.

3.4 Oxylipins level change in mice plasma

Several oxylipins from mice plasma were measured and listed in **Table 1**. The table consists of the change of 12 different oxylipins from three enzymatic pathways. For the mice fed with ω -6 enriched diets, we did not see a significant reduction in PGE2, PGD2,

and PGF2a when treating with TCDD versus dioxane (without TCDD). The same trend can also be observed in TXB 2 and LTB 4. For 20-HETE, a level increase was observed in ω -6 fed group with TCDD treatment, but it is not significant. For EETs, their downstream diols increased in TCDD treated mice fed with ω -6 enriched diets. It is interesting to notice that the only EET with significant change is 5,6-EET, which is decreased after TCDD treatment. No significant changes were observed from other EETs.

Table 1. Levels of oxylipin change in plasma.

Plasma Oxylipins (pmol/ml)	ω-6 enriched diet	
	-TCDD-TPPU	+TCDD-TPPU
PGE2	0.6 \pm 0.2	0.8 \pm 0.1
PGD2	0.5 \pm 0.1	0.7 \pm 0.1
PGF2a	2.1 \pm 0.7	2 \pm 0.2
TXB2	28.3 \pm 9.5	38.2 \pm 5.5
LTB4	0.6 \pm 0.4	3.6 \pm 2.3
20-HETE	0.3 \pm 0.1	0.5 \pm 0.1
5,6-EET	1431.3 \pm 418	734.2 \pm 130.4 *
11,12-EET	271.7 \pm 75.4	159.5 \pm 29.4
14,15-EET	183.5 \pm 52	104.9 \pm 20.9
5,6-DiHETrE	1.2 \pm 0.1	1.8 \pm 0.1 **
11,12-DiHETrE	0.8 \pm 0.1	2.2 \pm 0.3 **
14,15-DiHETrE	1.6 \pm 0.2	2.4 \pm 0.3 *

Plasma oxylipin levels were quantified (pmol/ml) for mice in four different experimental groups. Listed oxylipins are prostaglandins E2, D2, F2 α (PGE2, PGD2, and PGF2a), Thromboxane B2 (TXB2), Leukotriene B4 (LTB4), 20-Hydroxyecosatetraenoic Acid (20-HETE), epoxyecosatrienoic acids (EETs), and dihydroxyecosatrienoic acids

(DiHETrEs, the diols of EETs). The number after \pm represents the standard error. Highlighted red color means oxylipins level with significant change, * $p < 0.05$, ** $p < 0.01$

4. Discussions

4.1 Key findings

Using the tumor transplantation/metastasis model, we demonstrated that TCDD enhances the primary lung cancer metastasis to brain when fed with rich- ω 6 diet. This finding partially resembles our finding in a recently published paper that TCDD promoted the primary tumor growth and metastasis to the lung when mice are fed with rich- ω 6 diet¹³. The previously published studies from our group already broke a field in which TCDD may affect tumor growth and metastasis differently depending on the dietary contexts. This new ground can be further explored not only in lung metastasis but also in brain metastasis. The next step for this study is to compare the lung cancer metastasis to brain between ω -6 fed mice and ω -3 fed mice to further test if TCDD retards the metastasis when the mice are fed with ω -3 diet, but enhances metastasis when the mice are fed with ω -6 diet.

The results from immunohistochemistry and RT-PCR support the hypothesis that TCDD induces CYP 1A1 and CYP 1B1 expression in brain tissue when the mice are fed with ω -6 enriched diet. This finding is an important start to explore the influence of oxylipins on lung cancer metastasis to brain for several reasons: 1) CYP 450 are one of the three most important pathways to metabolize PUFA into downstream metabolites (Oxylipins).

2) Higher expression of CYP enzymes in brain can directly influence the level of oxylipins change in brain because TCDD and PUFAs have been proven to be able to pass the Blood-Brain Barriers (BBB)^{12,39}. 3) TCDD, as an AHR agonist, can act on cancer progression to brain differently based on different ratio of ω -6 or ω -3 enriched diets intake¹³. Previous research has revealed that a 1:1 ratio of ω -6/ ω -3 in the diet is the proper ratio of human evolution, and this ratio is recommended by nutritionists as a beneficial ratio as well^{40,41}. However, due to agricultural advance and industrial evaluation, the balanced ratio of 1:1 ratio of ω -6/ ω -3 in the diet has shifted to a high ω -6 content diet with the ratio of 20:1. The use of diet 21 in our study is to resemble the western diet ratio. Future research on CYP enzymes and diets will offer a new perspective on cancer prevention.

The plasma oxylipins of mice fed with ω -6 enriched diets demonstrate some interesting trends. EETs have previously been shown to be mitogenic and angiogenic in brain²³. In ω -6 fed mice, the lower level of EETs in the TCDD treated group contradicted with our hypothesis that TCDD enhances the level of EETs under ω -6 enriched diet.^{14,15} This might be because, without TPPU, plasma oxylipins are rapidly metabolized by epoxide hydrolase to diols. In the table, all the DiHETrEs significantly increased after TCDD treatment, but the potential mechanism for this change is not clear. The other interesting trend is that 20-HETE, which has an important role in breast cancer metastasis²³, increases with TCDD treatment in ω -6 fed mice, but the increase is not significant. Even though 20-HETE has not been heavily studied in brain metastatic cancers, this oxylipin can be studied more in the future.

For other oxylipins listed in table 1, they are primarily the products of the COX pathway and LOX pathway, which is not the focus in this paper. However, it will be valuable to show here for future investigations.

4.2 Limitations and future work

The method of harvesting the brain needs to be revised because the sagittal cut of brain collection will lead to some loss of metastatic evidence (RT-PCR half is unable to be evaluated for metastasis). In the future, we will not cut the whole brain into two pieces. Keeping the whole brain will help us see the location of metastatic lung carcinoma in brain. Besides, a morphology evaluation of LLC in brain H&E staining is not sufficient. We will identify some unique markers of LLC to differentiate from neuro cells. By doing so, we can confirm that the abnormal areas in brain H&E staining are LLC. Further, Due to limited time, H&E staining was only done in ω -6 fed mice. The ω -3 fed mice will be analyzed for metastasis in the future to observe the anti-cancer effect of ω -3 PUFAs and its metabolites.

Another further work is the immunohistochemistry analysis of CYP 1A1 and 1B1 expression, using the Aperio software to detect positive pixels of positive staining in a quantitative manner. This analysis is more accurate and objective than only presenting the pictures. In addition, female mice will be evaluated as well in comparison to male mice to see if sex plays a role in TCDD induction of CYP enzymes in brain under the same type of diet.

The plasma oxylipins data shows some huge variations, and some of the numbers present a high standard error as well. The repeat of the plasma oxylipins measurement is necessary to rule out the possibility that those trends are by chance. In addition, it would be more convincing and supportive for us to measure the oxylipins in brain directly because Oxylipins in plasma are decaying rapidly⁴². Brain oxylipins data will help us have a better visualization of the changes in brain, and this evidence will be more straightforward to link the changes to cancer progression.

5. Conclusions and implications

In conclusion, our data demonstrated that lung tumor brain metastasis was found in mice fed with rich- ω -6 diet in mice treated with TCDD as compared with untreated mice. Further, TCDD significantly induced CYP 1A1 and CYP 1B1 in mice brain tissue under ω -6 enriched diet. In addition, the levels of oxylipins demonstrated that epoxides 5,6 EET are increases after TCCD treatment, as well of different diols. The data presented in this study provided us a future research direction on combining effects of diets and environment carcinogens to analyze the mechanism to be involved in the metastasis to brain from the lung tumor cells.

Our study demonstrated a new mechanism in which the AHR activation and induction of CYP1 enzymes can enhance cancer metastasis from the lung to brain under typical western diet composition. Previous research has presented that CYP1 enzymes are capable of metabolizing environmental pollutants to cause cancer⁴³. In our study, we demonstrated in the recently published literature that CYP1 enzymes are metabolizing

PUFA, which can affect cancer¹³. Thus, CYP1 enzymes can be viewed as an intermediate player between AHR and cancer activity.

There are several implications of our main findings for future research. (1) The increasing CYP enzymes would metabolize the dietary PUFAs to oxylipins in the brain. (2) Alteration of certain types of oxylipins in the brain would be the potential mechanism to facilitate the metastasis of lung cancer brain metastasis. (3) Depending on the different ratio of ω -3 to ω -6 PUFAs in diets, TCDD, as a carcinogen, may have a protective role for cancer.

6. References

1. de Groot PM, Wu CC, Carter BW, Munden RF. The epidemiology of lung cancer. *Transl Lung Cancer Res* 2018;7:220-33.
2. Zhang Z, Hatori T, Nonaka H. An experimental model of brain metastasis of lung carcinoma. *Neuropathology* 2008;28:24-8.
3. Juricek L, Coumoul X. The Aryl Hydrocarbon Receptor and the Nervous System. *Int J Mol Sci* 2018;19.
4. Okey AB. An Aryl Hydrocarbon Receptor Odyssey to the Shores of Toxicology: The Deichmann Lecture, International Congress of Toxicology-XI. *Toxicological Sciences* 2007;98:5-38.
5. Ju Q, Zouboulis CC, Xia L. Environmental pollution and acne: Chloracne. *Dermatoendocrinol* 2009;1:125-8.
6. Poland A, Glover E, Kende AS. Stereospecific, high affinity binding of 2,3,7,8-tetrachlorodibenzo-p-dioxin by hepatic cytosol. Evidence that the binding species is receptor for induction of aryl hydrocarbon hydroxylase. *J Biol Chem* 1976;251:4936-46.
7. Kolluri SK, Jin UH, Safe S. Role of the aryl hydrocarbon receptor in carcinogenesis and potential as an anti-cancer drug target. *Arch Toxicol* 2017;91:2497-513.
8. Hankinson O. The role of AHR-inducible cytochrome P450s in metabolism of polyunsaturated fatty acids. *Drug Metab Rev* 2016;48:342-50.
9. Murray IA, Patterson AD, Perdew GH. Aryl hydrocarbon receptor ligands in cancer: friend and foe. *Nat Rev Cancer* 2014;14:801-14.
10. Forgacs AL, Kent MN, Makley MK, et al. Comparative metabolomic and genomic analyses of TCDD-elicited metabolic disruption in mouse and rat liver. *Toxicol Sci* 2012;125:41-55.
11. Ishida T, Matsumoto Y, Takeda T, Koga T, Ishii Y, Yamada H. Distribution of 14C-2,3,7,8-tetrachlorodibenzo-p-dioxin to the brain and peripheral tissues of fetal rats and its comparison with adults. *J Toxicol Sci* 2010;35:563-9.
12. Jacob A, Hartz AM, Potin S, et al. Aryl hydrocarbon receptor-dependent upregulation of Cyp1b1 by TCDD and diesel exhaust particles in rat brain microvessels. *Fluids Barriers CNS* 2011;8:23.
13. Huerta-Yepez S, Tirado-Rodriguez A, Montecillo-Aguado MR, Yang J, Hammock BD, Hankinson O. Aryl Hydrocarbon Receptor-Dependent inductions of omega-3 and omega-6 polyunsaturated fatty acid metabolism act inversely on tumor progression. *Sci Rep* 2020;10:7843.

14. Diaz-Diaz CJ, Ronnekleiv-Kelly SM, Nukaya M, et al. The Aryl Hydrocarbon Receptor is a Repressor of Inflammation-associated Colorectal Tumorigenesis in Mouse. *Ann Surg* 2016;264:429-36.
15. Kawajiri K, Kobayashi Y, Ohtake F, et al. Aryl hydrocarbon receptor suppresses intestinal carcinogenesis in ApcMin/+ mice with natural ligands. *Proc Natl Acad Sci U S A* 2009;106:13481-6.
16. Simopoulos AP. An Increase in the Omega-6/Omega-3 Fatty Acid Ratio Increases the Risk for Obesity. *Nutrients* 2016;8:128.
17. Huerta-Yepez S, Tirado-Rodriguez AB, Hankinson O. Role of diets rich in omega-3 and omega-6 in the development of cancer. *Bol Med Hosp Infant Mex* 2016;73:446-56.
18. Yuan D, Zou Q, Yu T, et al. Ancestral genetic complexity of arachidonic acid metabolism in Metazoa. *Biochim Biophys Acta* 2014;1841:1272-84.
19. Zhang G, Kodani S, Hammock BD. Stabilized epoxygenated fatty acids regulate inflammation, pain, angiogenesis and cancer. *Prog Lipid Res* 2014;53:108-23.
20. Yang Y-M, Sun D, Kandhi S, et al. Estrogen-dependent epigenetic regulation of soluble epoxide hydrolase via DNA methylation. *Proceedings of the National Academy of Sciences of the United States of America* 2018;115:613-8.
21. Morisseau C, Hammock BD. Impact of soluble epoxide hydrolase and epoxyeicosanoids on human health. *Annu Rev Pharmacol Toxicol* 2013;53:37-58.
22. Gabbs M, Leng S, Devassy JG, Monirujjaman M, Aukema HM. Advances in Our Understanding of Oxylipins Derived from Dietary PUFAs. *Adv Nutr* 2015;6:513-40.
23. Borin TF, Angara K, Rashid MH, Achyut BR, Arbab AS. Arachidonic Acid Metabolite as a Novel Therapeutic Target in Breast Cancer Metastasis. *Int J Mol Sci* 2017;18.
24. Loh JK, Hwang SL, Lieu AS, Huang TY, Howng SL. The alteration of prostaglandin E2 levels in patients with brain tumors before and after tumor removal. *J Neurooncol* 2002;57:147-50.
25. Paoletti P, Chiabrando C, Gaetani P, et al. Prostaglandins in human brain tumors. *J Neurosurg Sci* 1989;33:65-9.
26. Tang MK, Sun YM, Qin LJ, Jia YS, Zhang T, Zhang W. [Effect of Aspirin on Brain Metastasis of Lung Cancer and Its Possible Mechanism]. *Sichuan Da Xue Xue Bao Yi Xue Ban* 2017;48:857-61.
27. Yousefi M, Bahrami T, Salmaninejad A, Nosrati R, Ghaffari P, Ghaffari SH. Lung cancer-associated brain metastasis: Molecular mechanisms and therapeutic options. *Cell Oncol (Dordr)* 2017;40:419-41.
28. Ferreira MT, Gomes RN, Panagopoulos AT, de Almeida FG, Veiga JCE, Colquhoun A. Opposing roles of PGD2 in GBM. *Prostaglandins Other Lipid Mediat* 2018;134:66-76.
29. Smith WL, Urade Y, Jakobsson P.J. Enzymes of the cyclooxygenase pathways of prostanoid biosynthesis. *Chem Rev* 2011;111:5821-65.

30. Svensson CI, Zattoni M, Serhan CN. Lipoxins and aspirin-triggered lipoxin inhibit inflammatory pain processing. *J Exp Med* 2007;204:245-52.
31. Denkins Y, Kempf D, Ferniz M, Nileshwar S, Marchetti D. Role of omega-3 polyunsaturated fatty acids on cyclooxygenase-2 metabolism in brain-metastatic melanoma. *J Lipid Res* 2005;46:1278-84.
32. Zhang C, Harder DR. Cerebral capillary endothelial cell mitogenesis and morphogenesis induced by astrocytic epoxyeicosatrienoic Acid. *Stroke* 2002;33:2957-64.
33. Panigrahy D, Edin ML, Lee CR, et al. Epoxyeicosanoids stimulate multiorgan metastasis and tumor dormancy escape in mice. *J Clin Invest* 2012;122:178-91.
34. Panigrahy D, Greene ER, Pozzi A, Wang DW, Zeldin DC. EET signaling in cancer. *Cancer Metastasis Rev* 2011;30:525-40.
35. Rose TE, Morisseau C, Liu JY, et al. 1-Aryl-3-(1-acylpiperidin-4-yl)urea inhibitors of human and murine soluble epoxide hydrolase: structure-activity relationships, pharmacokinetics, and reduction of inflammatory pain. *J Med Chem* 2010;53:7067-75.
36. Shi S, Yoon DY, Hodge-Bell K, Huerta-Yepez S, Hankinson O. Aryl hydrocarbon nuclear translocator (hypoxia inducible factor 1beta) activity is required more during early than late tumor growth. *Mol Carcinog* 2010;49:157-65.
37. Yang J, Schmelzer K, Georgi K, Hammock BD. Quantitative profiling method for oxylipin metabolome by liquid chromatography electrospray ionization tandem mass spectrometry. *Anal Chem* 2009;81:8085-93.
38. Yang J, Solaimani P, Dong H, Hammock B, Hankinson O. Treatment of mice with 2,3,7,8-Tetrachlorodibenzo-p-dioxin markedly increases the levels of a number of cytochrome P450 metabolites of omega-3 polyunsaturated fatty acids in the liver and lung. *J Toxicol Sci* 2013;38:833-6.
39. Obermeier B, Daneman R, Ransohoff RM. Development, maintenance and disruption of the blood-brain barrier. *Nat Med* 2013;19:1584-96.
40. Simopoulos AP. Evolutionary aspects of diet and essential fatty acids. *World Rev Nutr Diet* 2001;88:18-27.
41. Simopoulos AP. Importance of the ratio of omega-6/omega-3 essential fatty acids: evolutionary aspects. *World Rev Nutr Diet* 2003;92:1-22.
42. Liakh I, Pakiet A, Sledzinski T, Mika A. Modern Methods of Sample Preparation for the Analysis of Oxylipins in Biological Samples. *Molecules* 2019;24:1639.
43. Pelkonen O, Nebert DW. Metabolism of polycyclic aromatic hydrocarbons: etiologic role in carcinogenesis. *Pharmacol Rev* 1982;34:189-222.